Computational Models of the Nano Probe Tip for Static Behaviors

Shaw C. Feng, Theodore V. Vorburger, Che Bong Joung, Ronald G. Dixson, Joseph Fu, and Li Ma

National Institute of Standards and Technology

Gaithersburg, Maryland 20899

{shaw.feng, theodore.vorburger, che.joung, joseph.fu, ronald.dixson, li.ma}@nist.gov

Abstract

As integrated circuits become smaller and faster, the measurement of line width must have less uncertainty and more versatility. A common requirement for uncertainty is less than 10 nm. The industrial need for versatility is three dimensional scanning in order to measure the geometric shapes of walls and trenches. Atomic Force Microscopes (AFMs) are commonly used in laboratories for a range of critical measurements of dimensions demanded by the electronic industry. However, it is difficult to predict the measurement bias arising from the compliance of the AFM probe. The issue becomes particularly important in this situation where nanometer uncertainties are sought for measurements with dimensional probes composed of flexible carbon nanotubes, having diameters of 1 nm to 10 nm, mounted on AFM cantilevers. In order to estimate the probe deflections due to surface contact and the resulting dimensional biases and uncertainties, we have developed a finite element model for simulating the mechanical behavior of AFM cantilevers with carbon nanotubes attached. The finite element model was developed using commercially available software systems. Spring constants of both the nanotube and cantilever in two directions are calculated using the finite element method with known Young's moduli of both silicon and multi-wall nanotube as input data. Compliance of the nanotube-attached AFM probe tip may be calculated from the set of spring constants. This paper presents static models that together provide a basis to estimate uncertainties in linewidth measurement using nanotubes. In particular, the interaction between a multi-wall nanotube tip and a silicon sample is modeled using the Lennard-Jones theory. Snap-in and snap-out of the probe tip in a scanning mode are calculated by integrating the compliance of the probe and the sample-tip interacting force model. Cantilever and probe tip deflections and points of contact are derived for both horizontal scanning of a plateau and vertically scanning of a wall. The finite element method and Lennard-Jones model provide a means to analyze the interaction of the probe and sample, including actual deflection and the gap between the probe tip and the measured sample surface.

1. Introduction

In semiconductor manufacturing, the smallest feature sizes have been decreased below 65 nm. As a result, a new challenge has arisen in nanometrology: to measure widths of lines and trenches and especially their sidewalls, with an acceptable measurement uncertainty [Dixson et al. 2007]. High aspect-ratio probe tips, such as nanotube-attached and focused ion beam-sharpened tips, are used to cope with this new challenge [Griffith et al. 1993, Nguyen 2001]. One problem is that these sharpened tips deflect when bending forces are exerted. Bending of a high aspect-ratio tip under contact forces can introduce measurement bias in a linewidth measurement. For example, if the

net contact force is repulsive, the tip bends away from the surface with respect to the cantilever. If the cantilever deflection is used to sense surface contact, then the linewidth will be biased low in this case. Further, the probe-tip geometry and the deflection of the probe tip are additional sources of uncertainty. In the intermittent contact mode, the gap between the probe tip and the sample surface create yet another source of uncertainty. These sources have to be accurately estimated and included in the measurement.

Computational modeling of parts and their assembly has been available for discrete manufacturing for four decades. Using a Computer-Aided Design (CAD) [Mortenson 1985] system, a computer-based geometric model can be created to represent a physical probe with known dimensions. With boundary and load conditions and relevant material properties specified, the geometric model can then be meshed into small elements. This model becomes a finite element model. It can then be solved using the Finite Element Method (FEM) [Bathe 1996] for the static and dynamic behaviors of the physical probe. Hence, probe-tip deflections may be computed. The forces that are exerted on the probe tip are predicted using atomic force interaction theories, such as the Lennard-Jones model. Additionally, the gap between the tip and the sample surfaces can be calculated as the probe approaches the surface and deflections are induced. As a result, the measured point on the sample surface can be calculated.

This paper describes probe-tip modeling using both CAD and FEM systems for the characterization of the static behavior of a probe tip. The static behavior of the probe tip both as it approaches a sample top surface and approaches a side wall is analyzed. Further, snap-in and snap-out are calculated to find the region of probe instability. Lastly, the analysis results in an estimated measured point. Specifically, Section 2 provides an overview of results from previous work on geometric modeling and nano probe mechanics. Section 3 describes the probe modeling. Section 4 shows probe tip deflection curves for vertical and horizontal surface scanning. Section 5 analyzes the probe tip-to-sample surface interaction based on the Lennard-Jones theory. Section 6 concludes the computational modeling work and points out future directions.

2. An overview of the state of computational modeling in AFM

Both CAD modeling and Finite Element Analysis (FEA) have been applied in product design and analysis in the mechanical industry for four decades. With proper conversion of derived units, they can be applied to the modeling and analysis of AFM probe tips on the nanometer scale. The static and dynamic behaviors of a commercial AFM V-shaped probe have been analyzed previously using FEM [Chen et al. 2005]. Also, an analysis of stress in a cantilever beam has been performed using FEM [Bhushan et al. 2002].

In order to apply the available FEM systems, material properties of all the components of a probe have to be in place. Research results on nanotube and cantilever beam moduli have become available. For the moduli of single wall and multiwall nanotubes, results from experiments show that Young modulus is in the range of 0.7 to 6 Tera Pascal, primarily depending on the diameter of the nanotubes [Salvetat et al. 1999, Akita et al. 2000, Qian et al. 2002]. Usually, the smaller the diameter the higher the Young's modulus is if the material of the nanotube is pure and well formed, i.e., close to a straight tube.

With the geometry and material properties available, the interaction force between the probe tip and the sample surface needs to be modeled. A method of measuring deflections of an attached nanotube has been published for pico-Newton order forces using an AFM [Nakajima et al. 2004]. Results of Lennard-Jones models for nanotube and silicon-based sample have been published [Sarid et al. 1997, Cappella et al. 1999, Rutzel et al. 2002]. A specific Hamaker constant, such as 5 x 10^{-19} Joule, in the Lennard-Jones model was used to simulate the imaging of a nonmetallic sample surface with a metallic nanotube tip (Snow et al. 2002). Other similar Hamaker constants are also available [Sarid 1997]. These constants are relatively close and fall within a small range. Furthermore, the Lennard-Jones model and the deflection of an AFM probe with a silicon tip have been applied to analyze a NanoCaliper™ probe for its performance [McClure 2005].

The use of a nanotube attached probe as a nanoprobe has become popular because of its high resolution and high aspect ratio. It has been shown that nanotubes can be used in high vacuum, air, and in liquid for imaging of biological materials and semiconductors and for material property testing [Dai et al. 1996, Hafner et al. 2001, Bhushan et al. 2004].

Currently, images of nano probe tips are available; however, computational models of the probe and finite element analysis of the probe are rarely found. Lennard-Jones theories are frequently applied; however, the spring constants of the probe are primarily those of cantilever beams. The total spring constant of the beam, the silicon tip, and the attached nanotube needs to be better computed. Also important, the probe tip contact point on the sample surface has to be estimated.

3. Nano probe tip models

A physical probe with a Multi-Wall Carbon Nano-Tube (MWCNT)-attached tip provides a basis for developing computational models in CAD and FEM systems. Figure 1 shows a Scanning Electron Microscopy (SEM) image of a probe tip with a nanotube. The size and overhang of the nanotube can be calculated from a pair of SEM images taken at two orthogonal orientations of the probe. A computational model can then be developed to simulate the real probe.

Figure 1 goes here

The geometries of a cantilever and the associated silicon tip are usually available from the vendor, and their dimensions are on the product specification sheet. With the shape and dimensions of the cantilever, a silicon tip, and an attached nanotube, the geometric models of all the parts can be developed and assembled into a probe model using a CAD system.

Figure 2 shows a geometric model, created using ABAQUS [ABAQUS 2006]. The model is meshed and ready for the application of finite element analysis. The meshes are applied to individual parts, including the beam, the silicon tip, and the nanotube. Element sizes and types have to be chosen according to the shape and accuracy requirements.

Figure 2 goes here

A second finite element model, developed using ANSYS [ANSYS 2002], of an AFM probe also includes definitions of all the necessary boundary conditions, the specification of material properties of each part, part-part interfacing constraints, and loading conditions. The modeling results from both ANSYS and ABAQUS are consistent.

Figure 2 also shows the deflection distribution of a probe when there is a upward vertical force applied to the tip of the nanotube. The base of the cantilever is fixed. The force is in the nanoNewton (nN) range, and the deflection of the tip is in the nanometer (nm) range.

A design of an AFM probe with a MWCNT-attached is depicted in Figure 3. The beam size is 300 μm long, 40 μm wide, and 4 μm thick. The size of the nanotube is assumed to be 0.02 μm in radius and 0.6 μm in length. The tip of the nanotube is assumed to be a spherical end. The radius of a MWCNT can vary in radius over a wide range. See, for example, [Nguyen et al. 2002] where the MWCNT radius is about 4 nm, and [Fu et al 2005] where the MWCNT radius is about 40 nm. Assigned material properties including densities, Young's moduli, and Poisson ratios are in Table 1.

Figure 3 goes here

Table 1 goes here

4. Static Deflections

When the probe is sufficiently close to a sample surface, there is an attractive force between the tip and the surface. The force on the tip is vertical in the negative Z direction when the measured surface is horizontal, as shown later in Figure 10. The force is horizontal in the positive X direction when the measured surface is vertical, as shown in Figure 11. The coordinate system is shown in Figure 3. Either force causes deflections of both the nanotube and the cantilever beam, as shown in Figure 4. The displacement of the beam in the Z-direction is observable with the laser sensor in an AFM. The nanotube tip displaces in both X and Z directions; however, displacements of the nanotube are not observable from the optical sensor system in an AFM.

Figure 4 goes here

According to [Wong 1997], the average maximum bending strength for MWCNT is 14.2 ± 8.0 GPa, below which the tube is expected to deflect elastically. In our case, the length of the tube is about 600 nm, and the diameter is about 40 nm. With one end fixed, the maximum lateral force at the free end can be conservatively estimated to be 64.2 nN, the force equivalent to a maximum bending strength of 6.2 GPa (14.2 GPa – 8.0 GPa). Figure 5 shows forces within the ±6 nN range applied in the X direction versus deflections of the nanotube tip in both X and Z directions and the beam deflection in the Z direction. Since the probe deflects elastically within the ±6 nN range, the deflection vs. force curve is a straight line. There are three lines, representing three different spring constants. They are spring constants of the nanotube deflecting in the X direction, the nanotube deflecting in the Z direction, and the beam deflecting in the Z direction. The slopes of these three lines are the values of the spring constants, as in Table 2.

Figure 5 goes here

Table 2 goes here

Similarly forces applied in the Z direction to the nanotube versus deflections of the nanotube in X and Z directions and the beam in the Z direction can be plotted, as shown in Figure 6. All three deflections are caused by the vertical force applied to the tip of the nanotube. Note that the deflection of the cantilever beam in the previous case, with the force in the X direction, is caused by the moment on the cantilever induced by the force.

Figure 6 goes here

Table 3 goes here

Lastly, the gravity causes both the beam and the nanotube to deflect. It is called the free state of the probe. The deflections are in Table 4.

Table 4 goes here

5. Modeling of tip-sample interaction

The probe tip-sample interaction is primarily described by the Lennard-Jones model on the nanometer scale. Since the probe tip is spherical and it is interacting with the sample surface, the Lennard-Jones force [Sarid 1997] can be defined as follows to approximate intermolecular forces interacting between the tip and the sample:

$$F_S(S) = \frac{HR}{6\sigma^2}\left(\frac{1}{30}\left(\frac{\sigma}{S}\right)^8 - \left(\frac{\sigma}{S}\right)^2\right) \qquad (1)$$

where F_S is the Lennard-Jones force and a function of S, S is the separation between the nanotube tip and the sample surface, H is the Hamaker constant (5.0×10^{-19} Joule), R is the radius of the nanotube, and σ is the separation at which the Lennard-Jones potential is null (0.3 nm). From Equation (1), the attractive force increases as the probe tip approaches the sample surface. As the attractive force increases, the cantilever beam will deflect more towards the surface. Figure 7 shows that the nanotube tip deflects in the Z direction more than the separation, i.e., Dtip_z is greater than S, as indicated by the solid curve. It means that the tip crashes into the surface. The observed beam deflection as the tip approaches the sample is indicated by the dashed curve. Similarly, as the probe tip is sufficiently close to a wall, the nanotube tip deflects more than the separation. The solid line in Figure 8 shows that the nanotube tip deflection in the X direction, Dtip_x, is greater than S as the tip is close enough to the wall, so the tip crashes into the wall. The dashed line indicates the deflection of the cantilever beam in the Z direction, Dbeam_z. Since the beam deflects in Z much less than the nanotube deflects in X, the deflection of the tip in the X direction is much less observable in the AFM optical sensor when the probe scans a wall than the deflection of the tip in the Z direction when the probe scans a horizontal surface.

Figure 7 goes here
Figure 8 goes here

To estimate how close the tip to sample distance is when the tip contact takes place, we perform an analysis of snap-in. Figure 9 shows that the effective spring constant of the combined cantilever and nanotube deflecting in Z is 3.02 nN/nm. From the derivative of the Lennard-Jones force curve F'(s), two separations S = 1.03 nm and S = 0.21 nm are the calculated distances where the spring constant of the system is equal to the slope of the Lennard-Jones force curve, as indicated as the intersection points Int1 and Int2 in the Figure. As the tip is closing to the surface, the tip starts to snap into the surface at the distance of 1.03 nm. As the contacting tip is pulled back from the surface, the tip starts to spring back to normal at the distance of 0.21 nm. This is the distance for snap-out. Between snap-in and snap-out, the region is unstable for the probe. The slope of the two dotted tangent lines on the Lennard-Jones force curve is 3.02 nN/nm, the spring constant.

Figure 9 goes here

Based on the deflections caused by the Lennard-Jones forces, the measured point can be estimated, assuming that no other factors contribute to the deflection of the beam

and the nanotube tip. Figure 10 shows that the deflections of the nanotube tip in both the X and Z directions can be calculated based on the deflection of the cantilever beam, using the information in Figures 6 and 7, and Table 4 if gravity is taken into account. The attractive force can be derived from the deflection of the beam. From the value of the derived attractive force, the gap between the tip and the sample can be calculated using the Lennard-Jones force curve. With the calculated gap and nanotube tip deflections, the estimated measured point can be calculated in the attractive force regime. Similarly as shown in Figure 11, the measured point on the wall can be estimated by calculating the gap, and the deflection of the nanotube tip in both the X and Z directions based on the deflection of the cantilever beam in the Z direction observed from the laser sensor.

<p align="center">Figure 10 goes here
Figure 11 goes here</p>

6. Conclusion

In practice, the probe tip is vibrating in the intermittent contact mode during scanning. The calculation of static deflections described above is an initial modeling step towards an analysis of probe vibration. The FEM modeling method is used to calculate deflections of the cantilever beam and the attached nanotube of a probe. FEM takes account of known material properties, component geometries, and boundary conditions. The attractive forces and deflections can be plotted to effectively calculate the spring constants of the tip or the beam and in either the X or Z direction. These calculated spring constants are then used measurement uncertainty estimation due to probe compliance.

With the attractive force model derived from Lennard-Jones theory and the calculated spring constants, the snap-in and snap-out distance of the probe tip to the sample surface can be estimated for either horizontal or vertical surface scanning. The region between snap-in and snap-out is unstable, i.e., the surface force gradient is greater than the effective spring constant in either the X or Z direction.

With calculated probe tip deflection and the calculated gap between probe tip and surface, the measured point can be estimated from the measured beam deflection, and read from the optical sensor system in an AFM. The estimated measured point for either horizontal or vertical surface depends on the spring constant for the attractive force in either the Z or X direction. Hence, a measured point can be estimated from the Lennard-Jones force. For future work, other possible factors that cause the probe tip to deflect, such as static electricity, Van der Waals forces, and hysteresis, need to be investigated. The results in this paper represent initial progress toward a thorough analysis of nanotube bending as well as a dynamic analysis for intermittent contact mode AFM.

Disclaimer: No approval or endorsement of any commercial product by the National Institute of Standards and Technology (NIST) is intended or implied. Certain commercial products are identified in this paper in order to facilitate understanding. Such identification does not imply that these products are necessarily the best available for the purpose.

References

1. ABAQUS/Standard, 2006, Theory and User's Manuals, release 6.6. ABAQUS, Inc., Pawtucket, RI, U.S.A.
2. Akita S, Nishijima H, Kishida T, and Nakayama Y, "Influence of force acting on side face of carbon nanotube in atomic force microscopy," Japan Journal of Physics, Vol. 39, 2000, pp. 3724 – 3727.
3. ANSYS Inc., *ANSYS 7.0 Documentation*, Canonsburg, PA: ANSYS Inc., 2002.
4. Bathe K, *Finite Element Procedures*, Prentice Hall, 1996.
5. Bhushan B and Agrawal G, "Stress analysis of nanostructures using a finite element method," Nanotechnology, Vol. 13, 2002, pp. 515 – 523.
6. Bhushan B, Kasai T, Nguyen C, and Meyyappan M, "Multiwalled carbon nanotube AFM probes for surface characterization of micro/nanostructures," Microsystem Technologies 10, 2004, pp. 633–639.
7. Cappella B and Dietler G, "Force-distance curves by atomic force microscopy," Surface Science Reports, Vol. 34, 1999, pp. 1 – 104.
8. Chen K and Huang J, "Analysis of Tip Effects on the Dynamic Characteristics of V-shaped Atomic Force Microscope Probes," Proceedings of the 2005 International Conference on MEMS, NANO and Smart Systems, 2005.
9. Dai H, Hafner J, Rinzler A, Colbert D, and Smalley R, "Nanotubes as nanoprobes in scanning probe microscopy," Nature, Vol. 384, No. 14, Nov. 1996, pp. 147 – 150.
10. Dixson R, Guthrie W, Cresswell M, Allen R, and Orji N, "Single Crystal Critical Dimension Reference Materials (SCCDRM): Process Optimization for the Next Generation of Standards," SPIE Proceedings, Vol. 6518, No. 651815, 2007.
11. Fu J, Dixson R, Orji G, Vorburger T, and Nguyen C, "Linewidth measurement from a stitched AFM image," Characterization and Metrology for ULSI Technology, edited by D. Seiler et al., American Institute of Physics, 2005.
12. Griffith J, Marchman H, Miller G, Hopkins L, Vasile M, and Schwaim S, "Line profile measurement with a scanning probe microscope," Journal of Vacuum Science and Technology B 11(6), Nov/Dec. 1993, pp. 2473 – 2476.
13. Hafner J, Cheung C, Woolley A, Lieber C, "Structural and functional imaging with carbon nanotube AFM probes," Progress in Biophysics and Molecular Biology, Vol. 77, 2001, pp. 73 – 110.
14. McClure P. and Mancevski V., "Calibration of a dual NanoCaliper ™ AFM for CD metrology," Proceedings of the SPIE Microlithography 2005 Conference, San Jose, CA, February 27 – March 4, 2005.
15. Mortenson M, *Geometric Modeling*, Wiley, 1985.
16. Nakajima M, Arai F, Dong L, and Fukuda T., "Calibration of carbon nanaotube probes for pico-Newton order force measurement inside a scanning electron microscope," Journal of Robotics and Mechatronics, Vol. 16, No. 2, 2004, pp. 155 – 162.
17. Nguyen C, Chao K, Stevens R, Delzeit L, Cassell A, Han J, and Meyyappan M, "Carbon nanotube tip probes: stability and lateral resolution in scanning probe microscopy and application to surface science in semiconductors," Nanotechnology 12, 2001, pp. 363 – 367.

18. Nguyen C, Stevens R, Barber J, Han J. and Meyyappan M, "Carbon nanotube scanning probe for profiling of deep-ultraviolet and 193 nm photoresist patterns," Applied Physics Letters, Vol. 81, No. 5, 2002, pp. 901 – 903.

19. Qian D, Wagner G, Liu W, Yu M, and Ruoff R, "Mechanics of carbon nanotubes," ASME Transaction Journal of Applied Mechanics Reviews, Vol. 55, No. 6, 2002, pp. 495 – 533.

20. Rutzel S, Lee S, and Raman A, "Nonlinear dynamics of atomic-force-microscope probes driven in Lennard-Jones potentials," Proceedings of Royal Society, A Vol. 459, 2003, pp. 1925 – 1948.

21. Sarid D, *Exploring scanning probe microscopy with Mathematica*, John Wiley & Sons, 1997.

22. Salvetat J, Andrew G, Briggs D, Bonard J, Bacsa R, Kulik A, Stockli T, Burnham N, and Forro L, "Elastic and shear moduli of single-walled carbon nanotube ropes," Physical Review Letters, Vol. 82, No. 5, 1999, pp. 944 – 947.

23. Snow E, Campbell P, and Novak J, "Atomic force microscopy using single-wall C nanotube probes," Journal of Vacuum Science and Technology B 20(3), 2002, pp. 822 – 827.

24. Wong E, Sheehan P, and Lieber C., "Nanobeam Mechanics: Elasticity, Strength, and Toughness of Nanorods and Nanotubes," Science, Vol. 277, 26 September 1997, pp. 1971 – 1975.
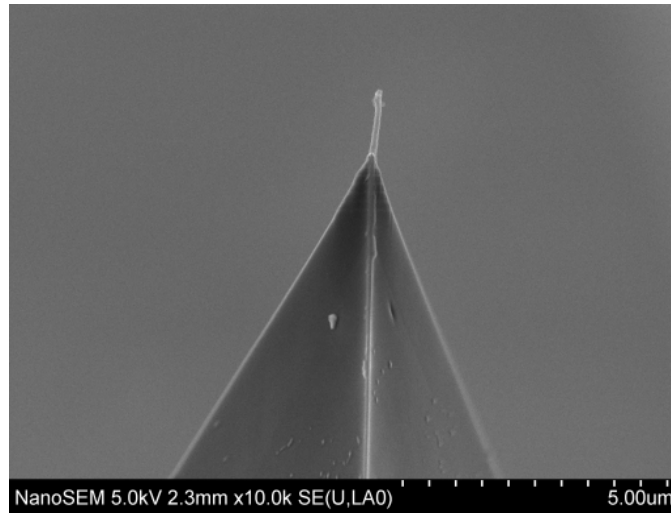
**Figure 1 Image of a nanotube-attached probe tip**
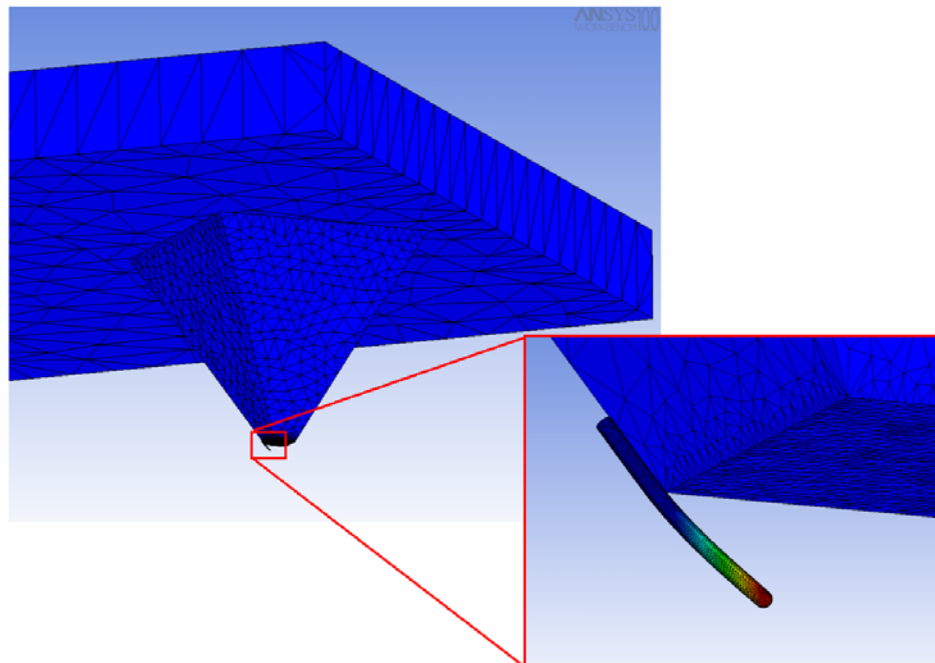

Figure 2 Finite element model of a probe.
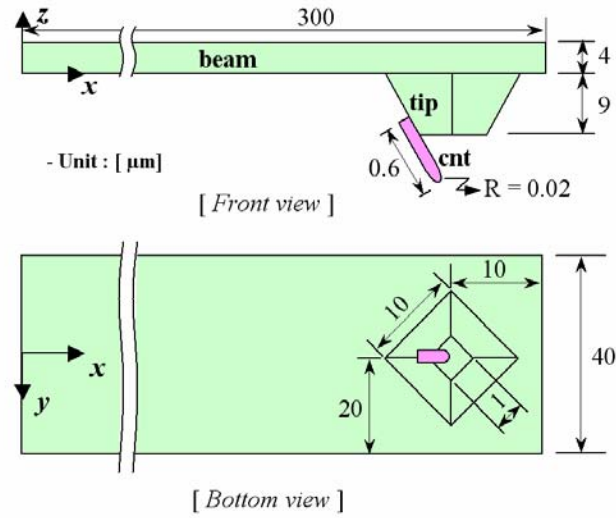
Figure 3 Dimensions of an example AFM probe in micrometers (not to proportion)

Table 1 Material properties

	Density [Kg/m^3]	Young's modulus[Pa]	Poisson's Ratio
Silicon Beam & tip	2.34E+03	1.50E+11	0.15
Nanotube	1.35E+03	1.20E+12	0.2
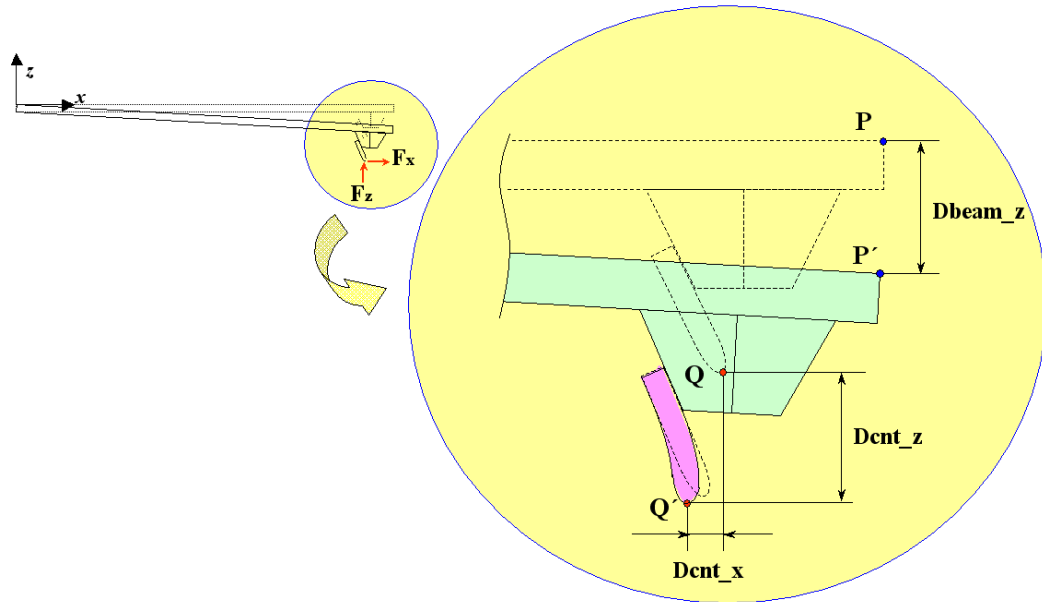
Figure 4 Nanotube and beam deflection.
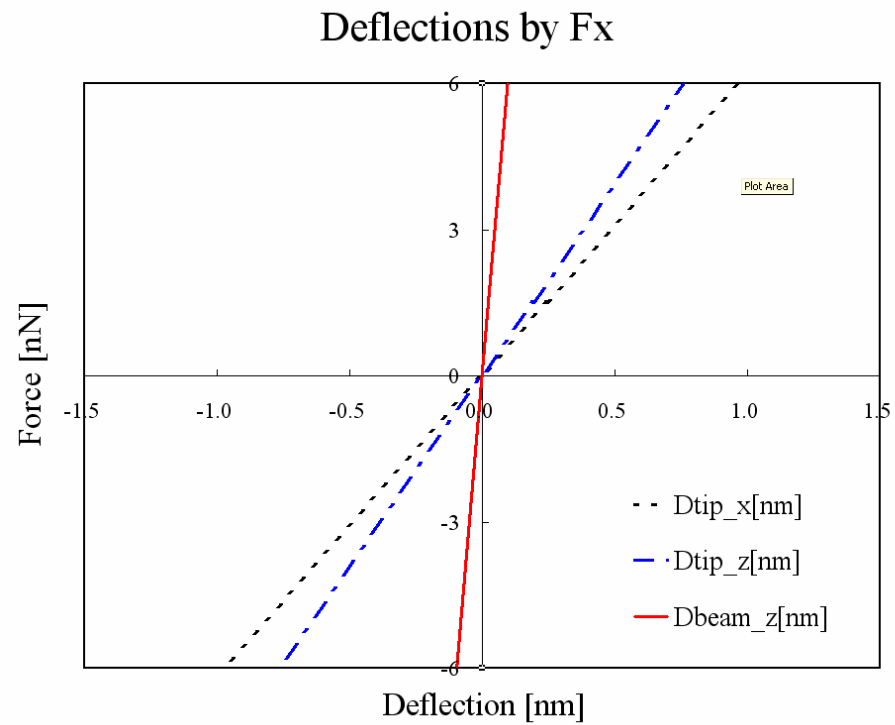
Figure 5 Force vs. deflection in X-direction

Table 2 Spring constants for wall scanning

Kx [nN/nm]	Dtip_x curve	Dtip_z curve	Dbeam_z curve
	6.2151E+00	7.9132E+00	6.3008E+01
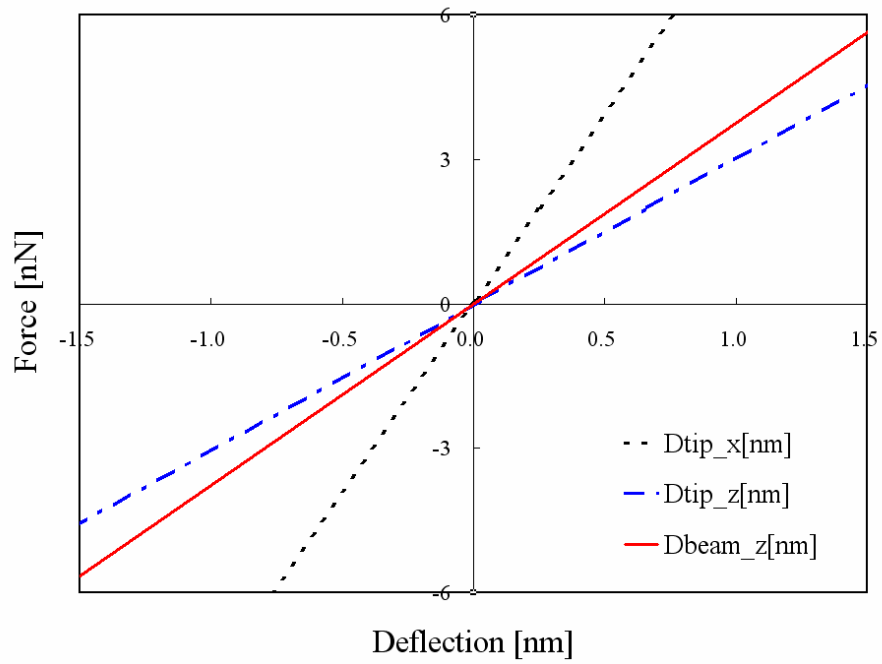
Figure 6 Force vs. deflection in Z-direction

Table 3 Spring constants for horizontal surface scanning

Kz [nN/nm]	Dtip_x curve	Dtip_z curve	Dbeam_z curve
	7.9138E+00	3.0192E+00	3.7658E+00

Table 4 Free state probe and tip deflections

Gravity[μm/s^2]	Dtip_x [nm]	Dtip_z [nm]	Dbeam_z [nm]
9.80066E+06	-5.9479E-03	-1.1219E-01	-1.1768E-01
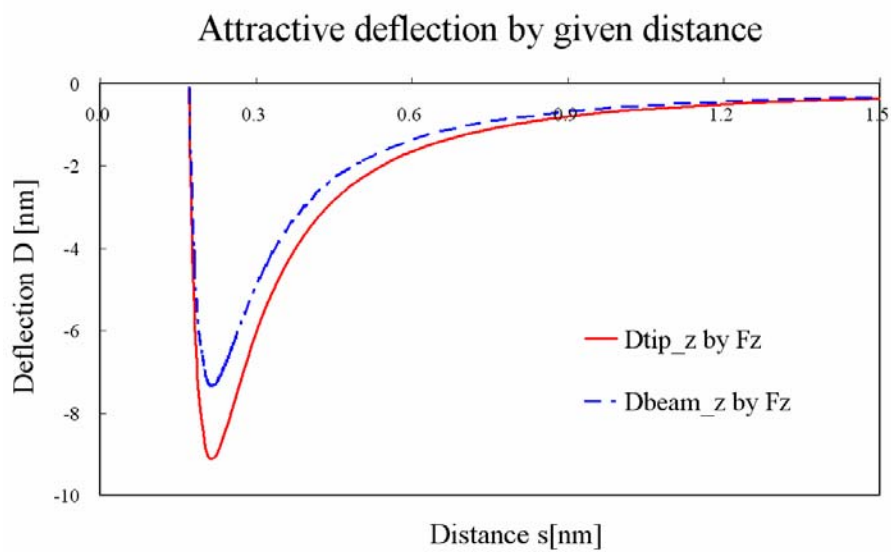
Figure 7 The beam deflection vs. separation in Z
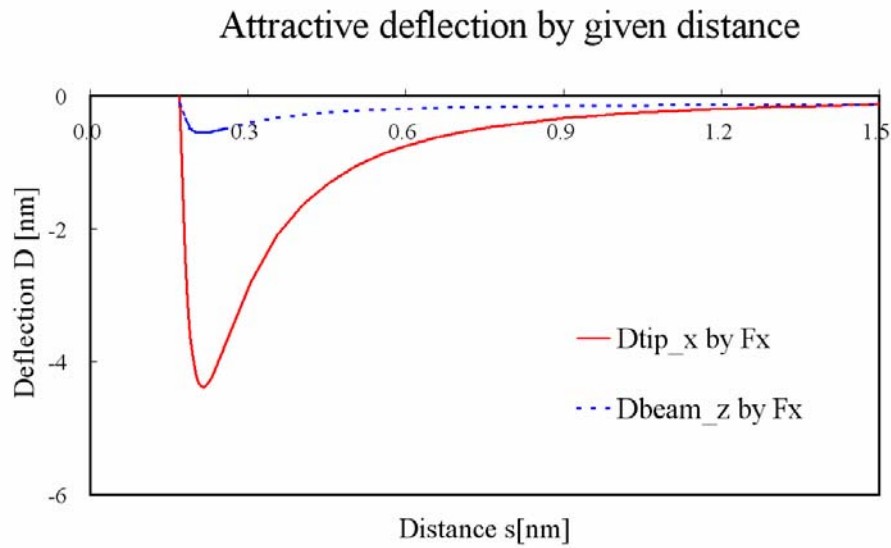
Figure 8 The beam deflection vs. separation in X
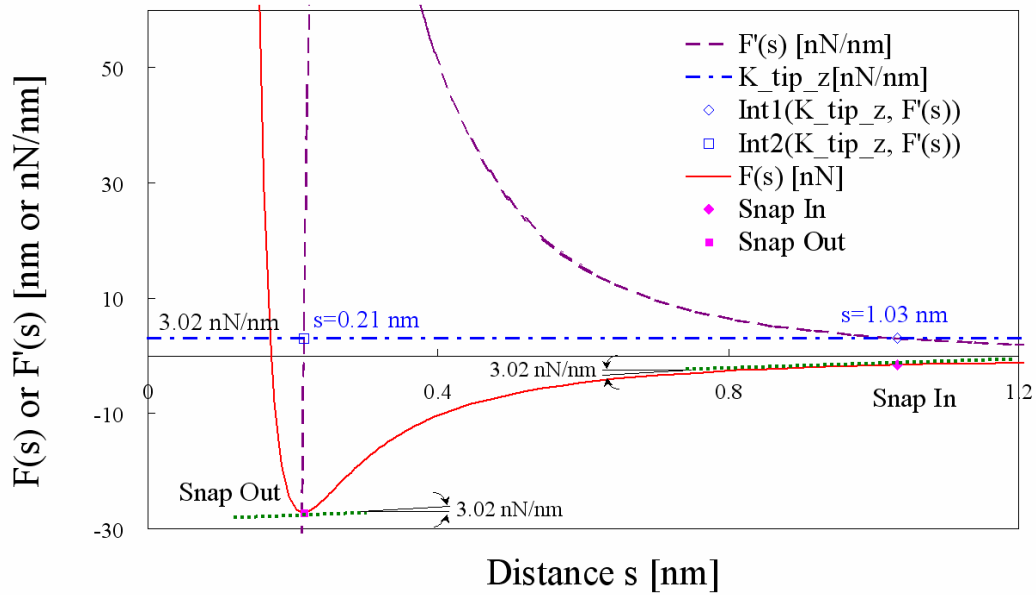

**Figure 9 Snap-in and snap-out analysis.**
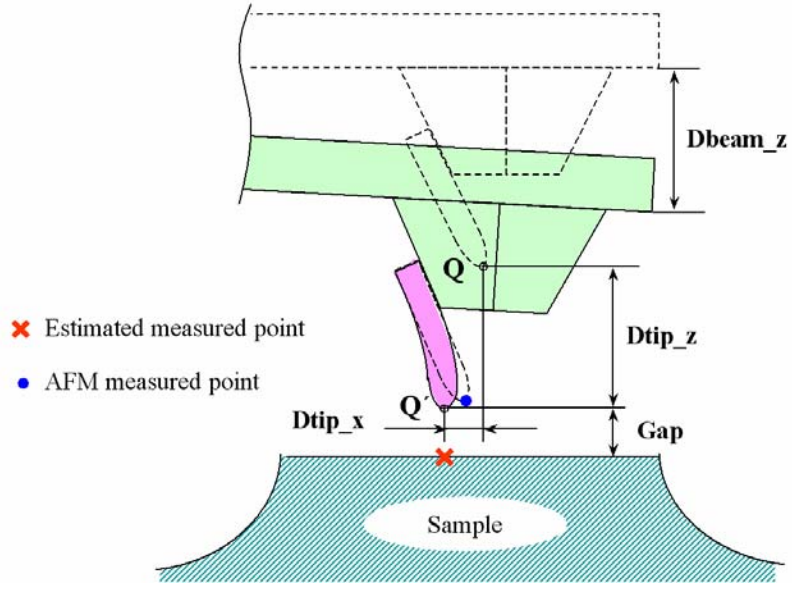
Figure 10 Estimated measure point - horizontal scanning
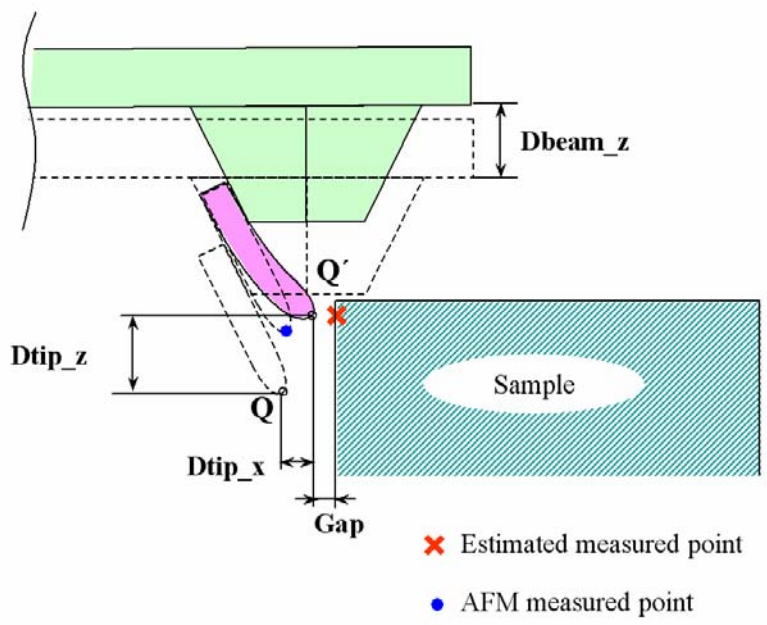
Figure 11 Estimated measured point in wall scanning